



Morphology and Instability of the Merapi Lava Dome Monitored by Unoccupied Aircraft Systems

15

Herlan Darmawan, Raditya Putra,
Agus Budi-Santoso, Hanik Humaida,
and Thomas R. Walter

Abstract

Episodic growth and collapse of the lava dome of Merapi volcano is accompanied by significant hazards associated with material redeposition processes. Some of these hazards are preceded by over-steepening of the flanks of the dome, its destabilisation, fracturing and gravitational collapse, producing lethal pyroclastic density currents. With the emergence of unoccupied aircraft systems (UAS), these changes occurring high up at Merapi can now be monitored at unprecedented levels of detail. Here we summarise the use of UAS at Merapi to better understand the evolution of the lava dome following the 2010 eruption. Systematic UAS overflights and photogrammetric surveys were carried out in 2012, 2015, 2017, 2018 and 2019, allowing identification of the

progression of major structures and a three-stage morphological evolution of the dome. We first highlight the significant morphological changes associated with steam-driven explosions that occurred in the period 2012–2014. A large open fissure formed and split the dome into two parts. In the years 2014–2018, hydrothermal activity dominated and progressively altered the dome rock. Lastly, in May–June 2018, a series of steam-driven explosions occurred and was followed by dome extrusion in August 2018, initially refilling the formerly open fissure. This work demonstrates the importance of reactivating pre-existing structures, and summarises the unique contribution realised by high resolution photogrammetric UAS surveys.

Keywords

Merapi · Lava dome · Unoccupied aircraft systems · Photogrammetry · Volcano monitoring

H. Darmawan (✉)
Laboratory of Geophysics, Department of Physics,
Faculty of Mathematics and Natural Sciences,
Universitas Gadjah Mada, Yogyakarta 55281,
Indonesia
e-mail: herlan_darmawan@mail.ugm.ac.id

R. Putra · A. Budi-Santoso · H. Humaida
Center of Volcanology and Geological Hazard
Mitigation, Geological Agency, Ministry of Energy
and Mineral Resources, Jalan Diponegoro 57,
Bandung 40122, Indonesia

T. R. Walter
GFZ German Research Center for Geosciences,
Telegrafenberg, Potsdam, Germany

15.1 Introduction

Lava domes often form above a volcanic conduit and in the summit region of a steep sided volcano due to cooling of viscous silicic magma extrusion (Calder et al. 2015). The extrusion of lava domes is associated with gradual and/or sudden changes of the morphology, may develop rockfalls and an

apron, cause over-steepening of the slope of the dome, and even trigger large-scale gravitational instability that can promote dome collapse. However, the collapse of an active lava dome is hazardous and difficult to monitor, as it can involve the flanks (i.e. a dome flank collapse) or even the inner core and the conduit (i.e. a dome sector collapse) to produce hot avalanches or pyroclastic density currents (PDCs). Due to the hazardous nature of the Merapi lava dome, Unmanned Aircraft System(s) (UAS) have become efficient to support the observation and the monitoring of geomorphological changes, to map structural lineaments and quantify volumetric changes, as well as to identify hydrothermal processes (Darmawan et al. 2018a, b). Therefore, UAS (other designations and common acronyms for UAS are: UAV, RPAS or simply *drones*) have become an essential tool for volcano monitoring in general (James et al. 2020) and for Merapi volcano in particular.

UAS have major advantages to standard airborne photogrammetric surveys and satellite imagery, as they are low cost, extremely high resolution and temporally highly flexible. Therefore, UAS have been used in different domains at volcanoes (James et al. 2020; Jordan 2019), including eruption volume estimations (Favalli et al. 2018), topographic change detection and geomorphic studies (Müller et al. 2017; Darmawan et al. 2020a; Wahyudi et al. 2020), gas and spectroscopic measurements (McGonigle et al. 2008), effusive eruption monitoring and large distance surveys exceeding 100 km range (Nakano et al. 2014), ash cloud imaging (Gomez and Kennedy 2018), and many other purposes such as sampling and carrying of specific instrumentations (Jordan 2019; James et al. 2020). Especially at explosive and dome-building volcanoes, the use of UAS is sharply gaining importance, as vividly demonstrated, during the eruption crisis at Gunung Agung (Syahbana et al. 2019), as well as during various episodes at Merapi (Darmawan et al. 2017; 2018a, b), mapping topographic changes at the flanks of Colima (Walter et al. 2018) or detecting rapid growth and collapse at the domes of Santiaguito (Zorn et al. 2020) and Fuego (Watson et al. 2017).

UAS have been systematically used at Merapi in the past decade by a number of organisations, institutes and scientists, including the National Institute of Aeronautics and Space (LAPAN), the Gadjah Mada University in Yogyakarta (UGM), the Geological Agency of Indonesia, and the Centre for Volcanology and Geological Hazard Mitigation (CVGHM), contributing to the general understanding of this well-studied volcano.

Merapi is a steep-sided dome building volcano that is frequently subjected to dome collapse producing PDCs due to gravitational failure and gas overpressure (Voight et al. 2000) and hosts a complex plumbing system at depth (e.g. Widiyantoro et al. 2018; Troll and Deegan 2023, Chap. 8). UAS were used to map deposits of major explosions on the lower flanks of the volcano and for post-disaster analysis (Rokhmana and Andaru 2016; Malawani et al. 2020), to map and monitor changes of the morphology and structure at the summit of Merapi (e.g. Darmawan et al. 2018a, b), and to assess the degree of hydrothermal activity (Heap et al. 2019). In this chapter, we review repeat measurements performed at the summit of Merapi to better understand the volcanic activity and associated landscape in the decade following the 2010 eruption.

The typical 4–6 year-long eruption cycle and dome building activity at the summit of Merapi (Voight et al. 2000) rapidly changed and ceased after the devastating 2010 eruption (Surono et al. 2012). Short term regrowth of the dome occurred immediately after the eruption, followed by a quiet and cooling-dominated phase for most of the years 2011 and 2012. Then a small steam-driven explosion occurred on 15 July 2012, which initiated a lasting series of explosions on 22 July 2013, 18 November 2013, 10 March 2014, 27 March 2014, and 20 April 2014. Heights of the eruptions were generally below 2000 m above the summit. The 18 November 2013 event was the biggest explosion in this series and formed a NW–SE oriented open fissure that dissected the lava dome into two parts as identified by synthetic aperture radar satellite (Walter et al. 2015). Afterwards, the activity has been dominated by

progressive hydrothermal alteration that weakened the dome structure and several rock falls that occurred in the period between 2014 and 2017 (Darmawan et al. 2018b). These rapid changes in activity were of very small scale, so that UAS provided the only detailed accounts to monitor them.

The value of an UAS is linked to the ability to cover areas that are otherwise beyond the reach of traditional observations. At Merapi, UAS are found useful especially in the steep and difficult-to-access summit crater and the regions between the lava dome and the deep crater. UAS overflights and photogrammetric records allowed us to track the renewed unrest that began in May 2018 after only very short precursory activity (BPPTKG 2018) and continued with steam-driven explosions in June 2018, which was then followed by new lava dome growth in August 2018. The morphology of the new dome gradually expanded due to continuous magma extrusion, steepening its slope that eventually were outflowing and collapsing to produce small volume PDCs (Kelfoun et al. 2021). We summarise the insights drawn from UAS surveys and compare the results with independent observations. We see strong evidence for a control of earlier structures on the Merapi lava dome, identify different stages of activity during the period 2012–2019, and systematically track the evolution of the lava dome, its morphology and instability.

15.2 Methods

15.2.1 Unoccupied Aircraft Systems (UAS)

A number of attempts were made before successful and systematic UAS overflights could be realised, exploring the performance (and failure) of kites, helikites, helium filled balloons, multi-copters and fixed wing UAS; many of these attempts ended in a crash of the device due to wind turbulence or other difficulties. Certainly, the requirements for UAS measurements at the lower flanks of Merapi are different from those

high up at the summit. UAS used at the lower flanks of the volcano, for many applications, can be small scale consumer drones (Jordan 2019). UAS used at the Merapi summit, in turn, are commonly of two types; (i) fixed-wing drones with a long reach that can be launched from large lateral and vertical distance (Rokhmana and Andaru 2016) and (ii) UAS that the pilot has to carry up to the summit, involving a 3–4 h car drive from Yogyakarta and a 3–4 h climb. The UAS used by us for the monitoring of the 2012–2019 dome activity at the summit involved different types, small and large, and with different specifications.

The fixed-wing UAS used in 2012 was a ~3 m-wide Skywalker 1680 V6 styrofoam UAS, which took off ~3 km from the summit, ascended to the programmed altitude and flew along a predefined path. The UAS carried a Canon S100 digital camera recording high quality images. The other and smaller UAS we carried up to the summit crater rim. These were standard consumer quadcopters, which were either DJI Phantom or DJI Mavic models. These included a Phantom 2, carrying a GoPro HERO 3 + camera and a H3-3D gimbal to reduce shaking (used in 2015), a Phantom 3 (used in 2017), a Phantom 4 (used in 2018) and a Mavic platinum quadcopter (used in 2019) for the recent flights.

To achieve high quality UAS records, we had to consider the weather conditions such as cloud, fog, wind, and fumarole activity. Therefore, every flight required very careful planning and spontaneous decision making. Launch sites were either on the upper eastern rim of the summit crater, or on lower elevations on the south flank of Merapi for the fixed-wing UAS (Fig. 15.1). The UAS flew at heights of 100–500 m above the dome, covered the Merapi summit area, and captured geotagged aerial images with intervals of 1–2 images/second on average. Thus, during each flight, hundreds of close-range nadir aerial images could be collected. These images were then analysed either for simple photo documentation or for three-dimensional (3D) point cloud reconstruction as described in the following section.

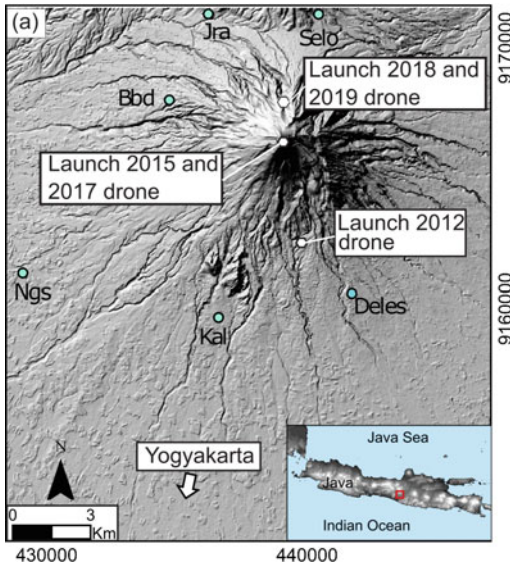


Fig. 15.1 Map of Merapi with drone launch sites

15.2.2 Photogrammetry and Structure From Motion (SfM)

To reconstruct the topography model of the Merapi lava dome, we applied the structure from motion (SfM) algorithm (Szeliski 2010), as implemented in the Agisoft Metashape Professional software. Some blurred and bad visibility images had to be removed before data processing as they can produce noise and outliers during 3D reconstruction. The 3D reconstruction using the SfM algorithm consisted of three main steps. First we applied the ground point detection and key point matching. After all objects were identified and matched, in the second step, we solved the intrinsic and extrinsic camera parameters, reconstructed a 3D scene, projected the identified objects into a 3D coordinate system and produced a 3D sparse point cloud. Then, by calculating the depth map of each camera frame, a 3D dense point cloud was generated in the third step. The generated 3D point clouds of the 2012, 2015, 2017 and 2019 aerial images collected over Merapi were compared to each other (using the Cloud Compare software) and then interpolated to produce high resolution digital elevation

models (DEMs) of the volcano summit. In addition, we also produced high resolution aerial photomosaic images of the Merapi lava dome. The repeat UAS surveys hence provide a sort of a time series of DEMs and orthomosaics (Derrien et al. 2020). These data were used to investigate the morphological and structural evolution of the Merapi lava dome from 2012 to 2019.

The data were represented and further analysed in the open-source geographical information system QGIS, allowing comparison of the DEMs and orthomosaics between the different episodes, before and after explosion, and delineation of the changes in the area. Using the GIS system, we also manually traced lineaments as identified by morphology or photographs. While results of the 2012, 2015 and 2017 flights were in part described in previous studies (Darmawan et al. 2018a; b; Heap et al. 2019), the latest results from 2018 and 2019 are new and reported here for the first time.

15.3 Repeat Surveys of the Summit of Merapi Using Unoccupied Aircraft Systems

We conducted the first successful UAS photogrammetry campaign at the Merapi summit on 26 April 2012, just a few months before the 15 July 2012 explosion. Then, we repeated the UAS flight campaign after the 2012–2014 explosion series, on 6 October 2015 and again on 2 September 2017. The new episode of lava dome growth that started on 18 August 2018 was first imaged by our drone on 23 September 2019.

15.3.1 Drone Flight 2012: Morphology and Structure of the Merapi Lava Dome

High resolution DEMs and aerial photomosaics derived from the 2012 UAS data mapped the morphology and structures of the lava dome and

provided the first and very important base map (Fig. 15.2), which also served as a reference for later surveys. The morphology of the 2012 lava dome was relatively flat-topped in shape and contained a large number of fissures and/or fractures (Fig. 15.2a, c). The dome had an E-W diameter of 154 m, and a N-S diameter of 145 m. The flat-topped surface area of the dome was estimated at 24,300 m², with abundant NW-SE

trending lineaments interpreted as fissures, fractures and other structural heterogeneities (Darmawan et al. 2018a). The lineaments had a mean azimuth of N135°E and an average density of 4 lineaments/m² (Fig. 15.2b). Lineaments at the dome margins were observed at preferred radial direction with respect to the centre of the dome, with a resolved common length ranging between 5 and 50 m.

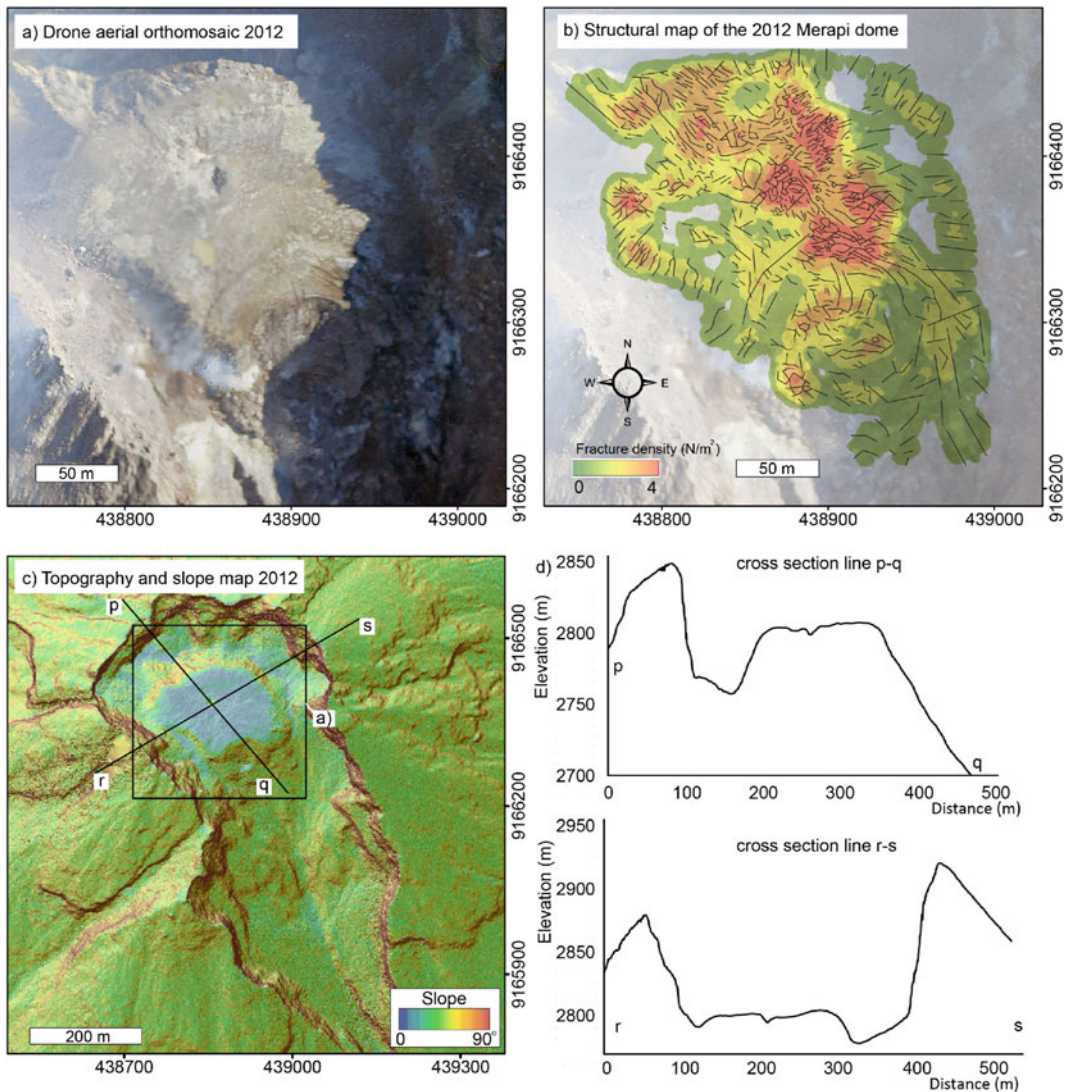


Fig. 15.2 a High-resolution aerial orthomosaic of the Merapi dome in 2012, showing detailed morphology. **b** Lineament distribution concentrating in the middle of the 2012 dome with NW-SE azimuth and 4 fractures/m².

c and d Slope map and topography profile indicating that the top of the 2012 Merapi dome was relatively flat, with a small depression in the middle, and steep sided with slopes $\sim >40^\circ$

More detailed topographic analysis of the dome revealed not only a flat-topped plateau but also a slightly convexly curved morphology at the top, forming a 50–70 m area that was slightly bowl shaped (Fig. 15.1), possibly associated with intense cooling of the dome since it had formed in 2010. A deep, possibly old vent was expressed with a maximum depth of 6 m and a diameter of 10 m, located approximately at the centre of the dome (Fig. 15.1c, d). The eastern, western and northern margins of the dome were steeply inclined with slopes of 43.8°, 32.2°, 42.9°, respectively, surrounded by blocky talus material forming the dome's apron (Fig. 15.1c, d). The southern part of the lava dome was steeply inclined at 40° or even more, with a blocky appearance, and showed sites of intense degassing (as seen by white steam in the imagery) especially in the western area of the southern flank. As the southern slope was steep and unbuttressed, it represented the sector of the dome most prone to instability and gravitational collapses (Darmawan et al. 2020b, c). A small-scale localised horseshoe shaped structure can be delineated on the southern dome sector.

15.3.2 Drone Flight 2015: Changes Associated with Steam-Driven Explosions

A series of steam-driven explosions that occurred between 2012 and 2014 partially split the carapace of the dome, as observed by satellite radar observations (Walter 2023, Chap. 14). The explosions were monitored by the Merapi Volcano Observatory staff (BPPTKG), describing (a) the first explosion on 15 July 2012, which ejected at the NE part of the dome, (b) a second explosion on 22 July 2013, which removed part of the NE dome again, and (c) the largest explosion on 18 November 2013, which was associated with a new NW–SE trending fissure that split the dome into two parts. This was followed by smaller explosions on 10 March 2014, 27 March 2014, and 20 April 2014. The changes due to these explosions are concentrated around

the fissure area, so that our high resolution UAS data provided more detailed records.

The following UAS dataset was acquired in October 2015 (one year after the 2012–2014 eruptions) and allowed quantification of the morphological changes associated with the explosion series in much greater detail. The NW–SE trending open fissure could be mapped at centimetre-scale resolution from our DEM and aerial orthomosaic (Fig. 15.3). The surface of the lava dome was covered by boulders and angular blocks with diameters of up to ~7 m, and by volcanic tephra accumulating to a thickness of ~3 m as determined by the difference of the two DEMs (Fig. 15.3a). The open fissure did not display signs of an displacement but was fractured with a mean azimuth of N135°E, which is consistent with the azimuth of the lineament as observed in the first UAS survey conducted in 2012 (Fig. 15.3b). The actively degassing area at the southern part of the dome evolved to a crescent-like or horseshoe-shaped structure, open to the south (Figs. 15.1b and 15.3b). The structure, first identified in the 2012 aerial image, has deepened up to 8 m depth and delineated a destabilising block (Darmawan et al. 2018b).

The main NW–SE trending fissure was steeply inclined, often vertical and had a maximum depth of ~33 m, a width of 28 m, and a length of ~95 m (Fig. 15.3c, d). The deepest part of the open fissure was found to be located at the depression already identified in the 2012 UAS data, representing remnants of an older vent (Fig. 15.3 d). This underlines the structural importance of earlier structures (here: a pre-existing vent) and their possible relevance for understanding later stages of dome building activity.

15.3.3 Drone Flight 2017: Changes Associated with Hydrothermal Activity

Following the 2012–2014 explosions, the activity of the Merapi dome was dominated by almost 4 years of degassing activity and virtual absence

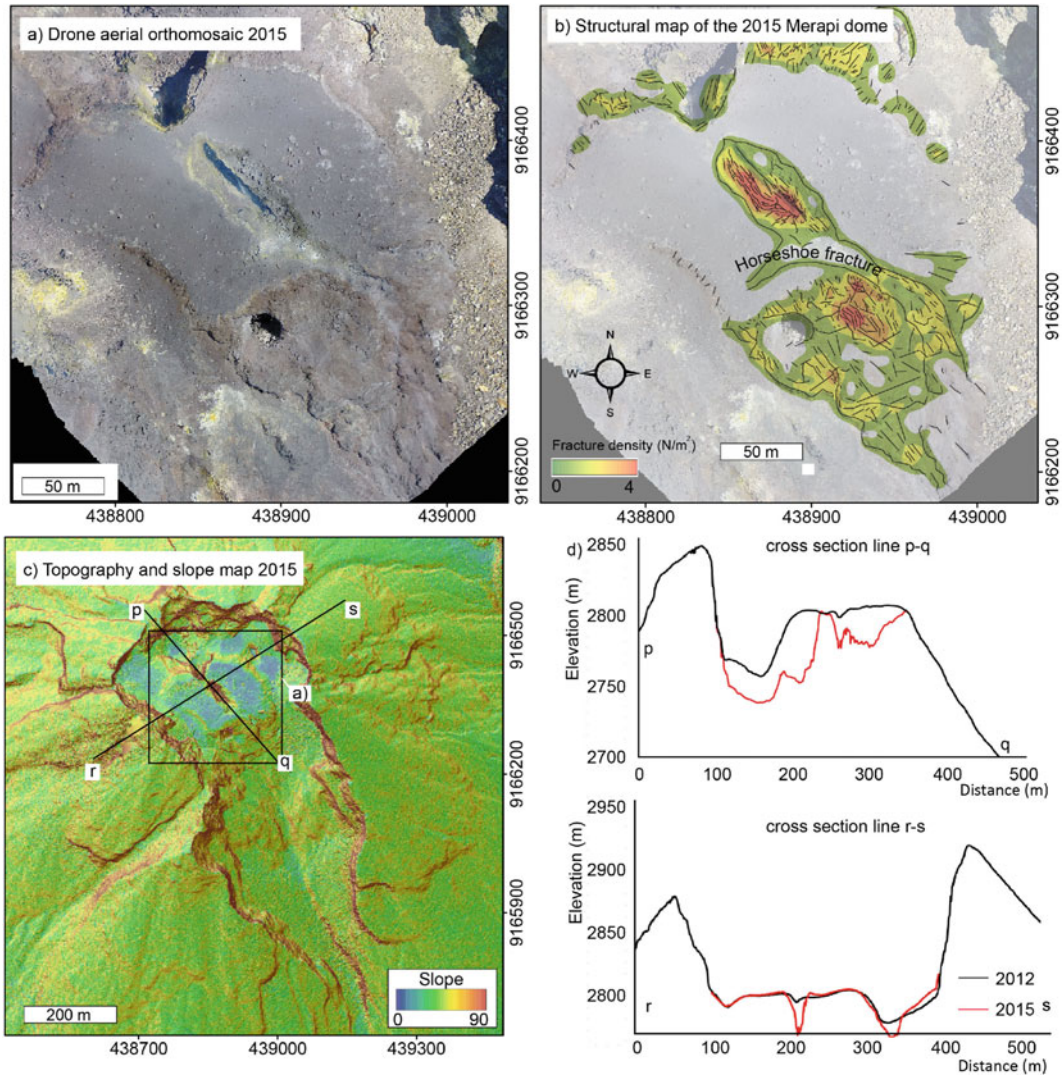


Fig. 15.3 **a** High resolution orthomosaic of the 2015 Merapi dome clearly showing the significant changes of the Merapi dome due to the 2012–2014 steam explosions. **b** Open fissures formed in the middle of the Merapi dome

with abundant NW–SE oriented fractures that were already identified in our 2012 UAS orthomosaic data. **c** and **d** Slope map and topography profiles suggesting that the fissure is near vertical and ~ 33 m deep

of large explosions (Fig. 15.4), as also confirmed by volcano observatory records. The UAS overflight carried out in 2017 showed intense and ongoing hydrothermal activity, but no major morphological changes except for small scale rock falls. A comparison of the 2017 and the earlier 2015 UAS dataset helped to identify rockfalls at steep cliffs often at a location that was also characterised by strong steaming and yellowish colourisation associated with

hydrothermal activity (Fig. 15.4c), further described in Heap et al. (2019) and in Darmawan et al. (2022). Moreover, five fractures with diameters of 0.3–1.3 m and located at the crescent-like structure were found to have intensified their degree of degassing and yellowish colourisation (Fig. 15.4c), although the plume and hydrothermal colourization can be influenced by the time of the day of the survey and atmospheric condition. Therefore,

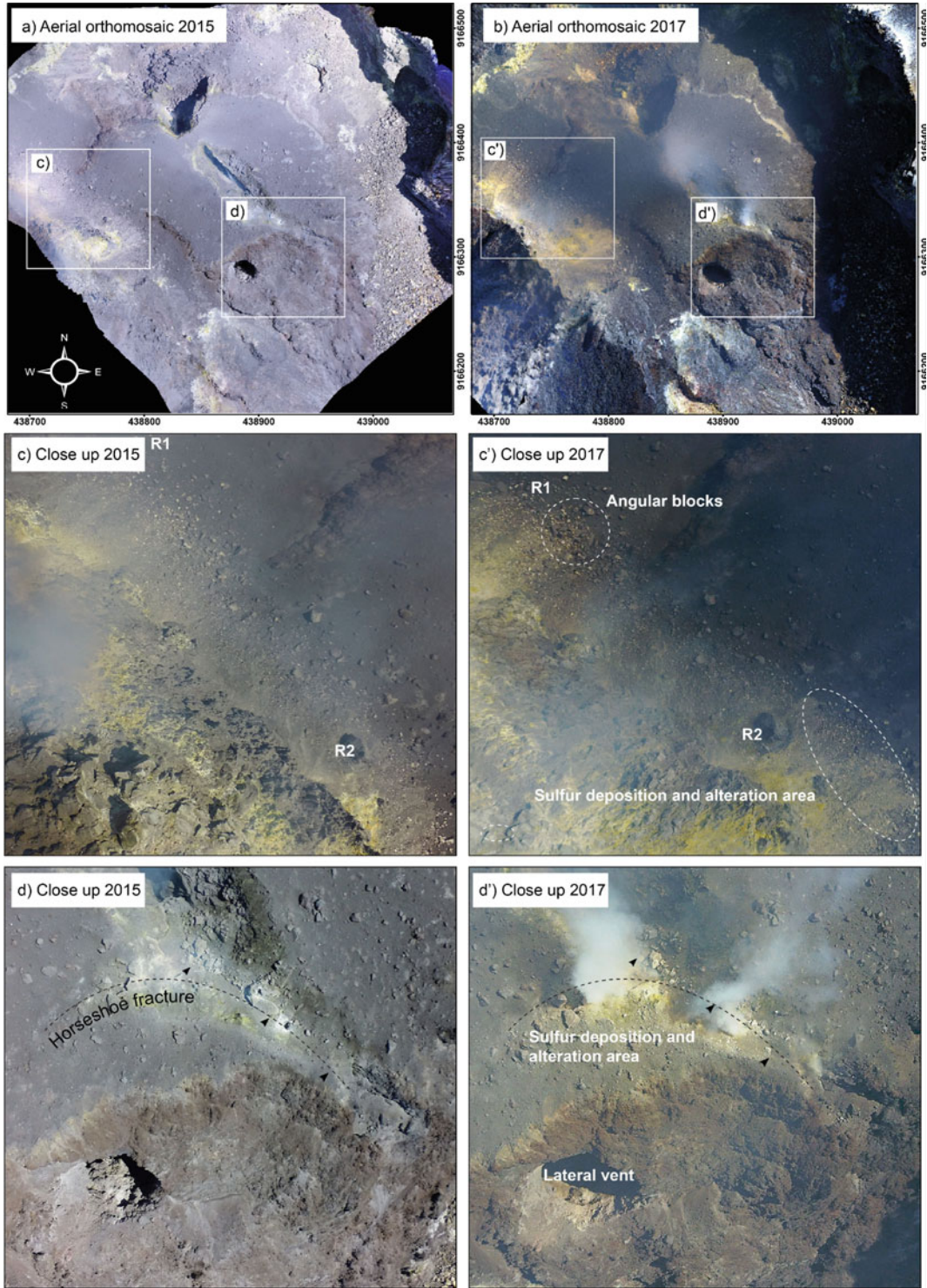


Fig. 15.4 Progressive hydrothermal alteration of the Merapi lava dome between **a** 2015 and **b** 2017. **c** and **c'** Zoomed images at the western cliff area showing evidence of hydrothermal alteration that weakens the rock and

triggers rock falls (red circle). **d** and **d'** Hydrothermal alteration also progressively occurred at the fractures of the southern part of the dome, which is indicated by the yellowish rock colour (black arrow)

hyperspectral analysis may be a better technique to document such activity (Kereszturi et al. 2018). As hydrothermal alteration can weaken the rock strength, we have speculated that the degassing and associated hydrothermal alteration can progressively trigger gravitational dome failure in the future (Darmawan et al. 2018b).

15.3.4 Drone Flight 2019: Changes Associated with a New Dome Growth Episode

After ~ 4 years of quiescence, a new series of steam-driven explosions occurred between May and June 2018. The first explosion occurred in the morning of 11 May 2018, when hikers were enjoying the sunrise at Merapi summit (as reported by BPPTKG), underlining the high-risk potential of the volcano. Fortunately, no victims were reported as the volcanic ejecta were dominated by fine grained tephra. Further explosions followed on 21, 22 and 23 May and on 1 June 2018, with maximum eruption column heights up to ~ 7 km above the summit. As the eruptions were getting more energetic, the alert level was raised to level 2 (Waspada) on a scale from 1 to 4.

The UAS data obtained by BPPTKG in August 2018 allowed us to illustrate the initiation of dome growth that started soon after the steam-driven explosions. The main dome growth started precisely inside the NW–SE trending open fissure that formed more than 4 years before and was most pronounced at a location where the NW–SE trending fissure was widest and where UAS data already showed a vent location as early as 2012 (see also Fig. 15.2). The morphology of the new dome during early emplacement was first elongated along this NW–SE trending fissure, with a length of ~ 55 m, a width of ~ 18 m, and an area cover of ~ 800 m² (Fig. 15.5). Continuous magma extrusion gradually changed the morphology of the lava dome as shown by a cross section determined by further UAS surveys on 12 August 2018 and 9 April 2019 (Fig. 15.6). The outline of the dome changed from being confined inside the fissure to a symmetric shape

with a blocky surface that consisted of some lava dome lobes. Comparison of the 2018 and 2019 UAS data further showed that during the first dome emplacement episode, the elevation of the dome was $\sim 2,860$ m, which then gradually increased to $\sim 2,875$ m and covered the entire surface area of the formerly flat-topped dome mapped in 2012 and 2015.

The final morphology of the new dome emplacement was half spherical (red polygon in Fig. 15.5), almost symmetrical, with blockier surface texture. Closer observations indicate, however, a rather episodic nature of dome emplacement, as it consisted of several individual lava lobes that piled up, possibly shear lobes and some crease structures, each hosting abundant and characteristic lineaments, allowing the different lobes to be distinguished (Fig. 15.5). By April 2019, the dimension of the new dome extrusion was $\sim 170 \times 160$ m, covering an area of 24,700 m² (Fig. 15.5b, d).

Several forms of mass wasting continued to be detectable by UAS data. Small gravitational collapses firstly occurred at the north-eastern part of the dome already in 2018, causing some debris at the northeast side of the crater infilling the depression between the dome and the crater wall (Fig. 15.6). Later collapses occurred predominantly in southerly directions. A major collapse, evident in 2019 UAS data (Fig. 15.5), was characterised by a crescent-like structure located at the steep southern flank part of the Merapi lava dome, which suggests continued dome instability due to gravitational instability at this site (Darmawan et al. 2020b). We note that this is the site of previous instability and crescent-like fracturing identified already in the 2012, 2015 and 2017 data. The instability can even be identified by simple camera monitoring networks operated on the southern flank that show the occurrence of rock falls (Fig. 15.7). As the rocks are falling and colliding, they break into smaller pieces within seconds that increase their velocity up to ~ 90 m/s (Darmawan et al. 2020c), further fragmenting to produce small (granular or pyroclastic) flows. Such short-term changes are beyond the ‘eyes’ of our campaign UAS surveys.

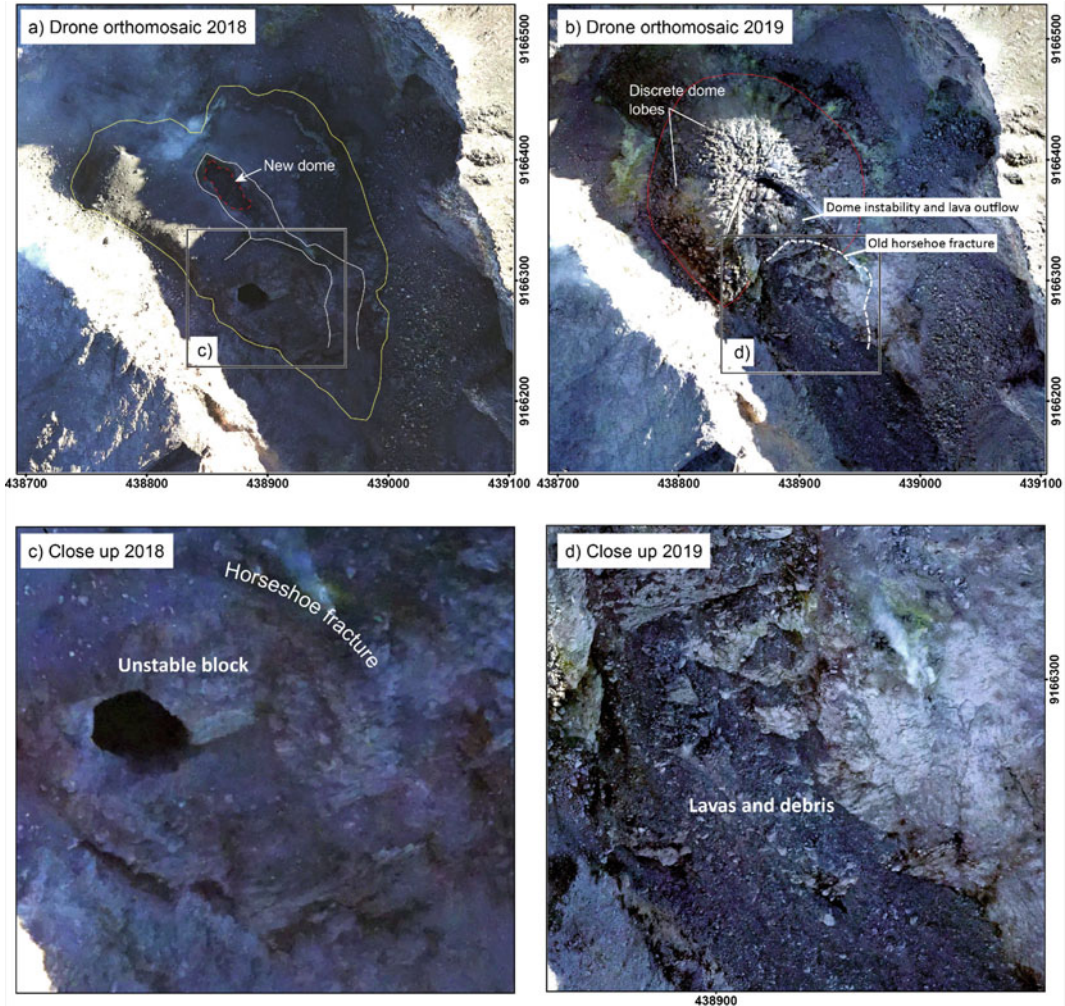


Fig. 15.5 **a** Morphology of the new lava dome, identified by our UAS camera on 12 August 2018, showing that the dome has an elongated shape and grew at the fissure area. **b** One year later, the dome has a half spherical, relatively symmetrical shape, and our UAS camera

observed a collapse area at the southeastern part of the dome, which is delineated by a horseshoe-shaped structure. **c** and **d** Close-up view of the southern part of the dome showing an unstable block in 2018 that collapsed in 2019, possibly caused by hydrothermal alteration

15.4 Monitoring Lava Dome Building Activity and Morphological Changes in the Summit Area of Merapi Using Repeat Unoccupied Aircraft Systems Surveys

UAS based photogrammetric data allow observation at high resolution, showing details of morphological and structural features of the lava

dome of Merapi volcano. Here we reviewed findings from repeat UAS surveys conducted by us in the summit region of the volcano and compared these to independent observations made by the volcano observatory (BPPTKG).

We find evidence for a structural memory, whereby older dome structures further evolve, affect or even control the later development of the lava dome (Darmawan et al. 2022). This structural influence involves (i) a small explosion vent that is also the location of the later NW–SE

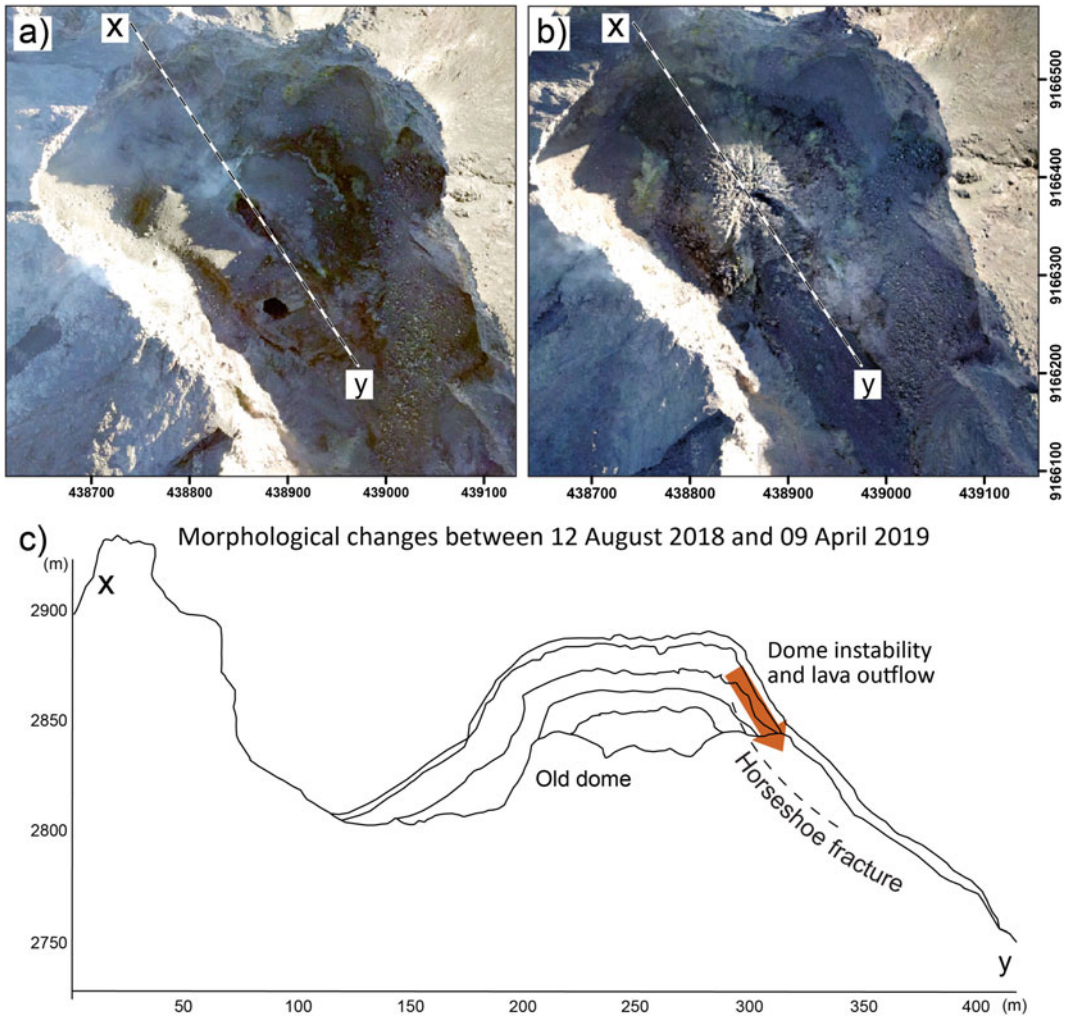


Fig. 15.6 Aerial images of Merapi summit that were acquired between **a** August 2018 and **b** April 2019, illustrating the evolution of the Merapi lava dome growth due to continuous magma extrusion. **c** Cross sections of line *x*–*y* during dome emplacement record the

morphological changes in a NW (left) to SE (right) direction. The initial dome filled the fissure area in August 2018, gradually expanded symmetrically, and finally filled in the crater of Merapi

trending fissure, (ii) the widest section of the NW–SE trending fissure that is also the site of the new dome growth initiation, (iii) a crescent-like fracture that is also the location of a later dome collapse and lava extrusion, and (iv) fumarole activity at steep flanks that are also the sites of later rock falls. We therefore conjecture that reactivation of pre-existing structures play an important role for the evolution of the lava dome, which is also consistent with observations made elsewhere (Watts et al. 2002; Ashwell et al. 2018).

The morphology of the Merapi dome has changed significantly due to several geological processes between 2012 and 2019. Prior to the 2012–2014 steam-driven explosions, the dome morphology was controlled by dome emplacement, cooling and volumetric expansion causing radial fractures at the dome margin and a flat-topped plateau dissected by NW–SE oriented lineaments. Between 2012 and 2014, the dome morphology changed due to six steam-driven explosions that commonly occur during the rainy

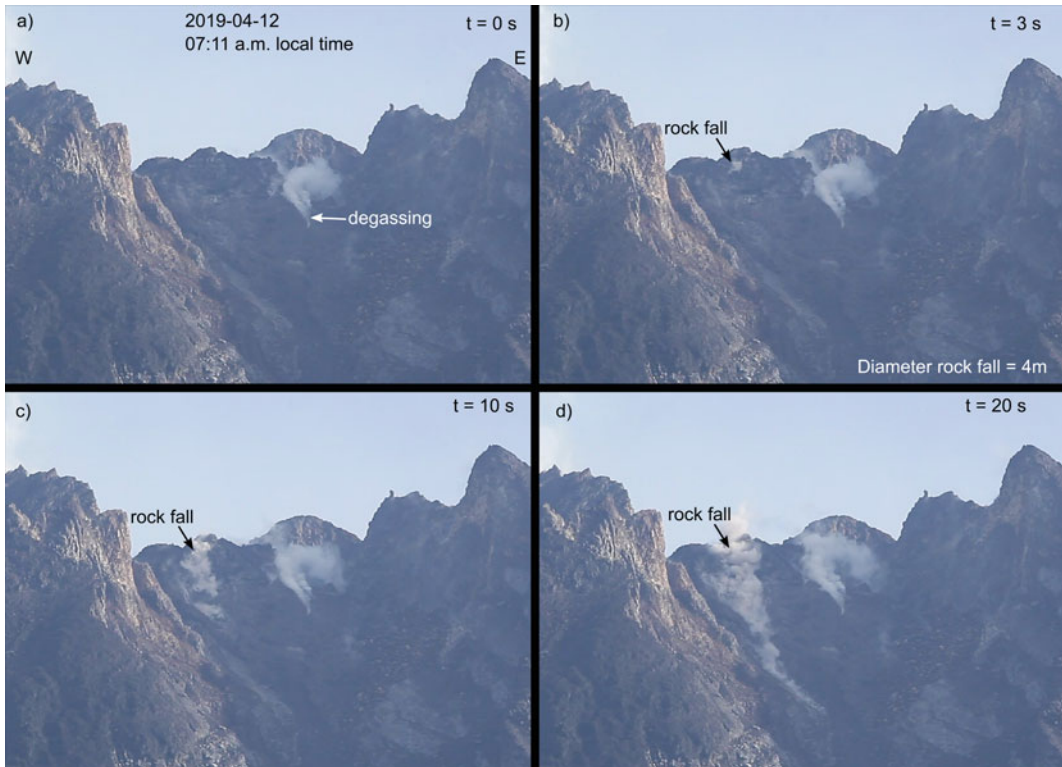


Fig. 15.7 Mechanism of a discrete rockfall of the lava lobe at the Merapi lava dome recorded by our high-resolution camera on 12 April 2019. **a** and **b** In the first 3 s, the rock was subjected to gravitational free fall. **c** Within 10 s, it then collided and broke into several rock

fragments. **d** The velocity of the rockfall was terminated over a sandy area (~ 200 m from the summit) in the next 10 s. Rockfalls occurred frequently as magma continuously extruded in the southeastern part of the dome

season. The explosions opened a large NW–SE oriented and open fissure that dissected the dome into two parts. As the UAS data reveal the presence of larger blocks closer to the fissure, and as no major displacement was found in association with its formation (Walter et al. 2015), it can be speculated that it is rather an elongated eruption fissure than a structure associated with strong deformation. The location of the NW–SE trending open fissure is confined to the sites of NW–SE oriented fractures identified in the 2012 UAS dataset, suggesting a structural control of the pre-existing fractures.

Steam-driven explosions might be caused by interaction between rainwater and the hot dome interior. UAS data at Merapi provided the necessary DEM resolution to study how rainwater may accumulate and possibly percolate through

the identified fractures, where it interacts with the hot dome interior, causing shallow hydrothermal gas overpressure and steam-driven explosions (Darmawan et al. 2018a). The NW–SE trending fissure at the Merapi dome is possibly related to a regional tectonic trend seen in the volcanic chain of Merapi—Merbabu—Telomoyo—Ungaran (Walter et al. 2015; Bronto et al. 2023, Chap. 7; Harijoko et al. 2023, Chap. 4). The NW–SE oriented lineaments mapped from our 2012 UAS data were identified previously (Beauducel et al. 2000), suggesting that this trend at Merapi is relevant in the long-term. Strong contrasts in seismic velocities also suggest a significant role of vertical heterogeneities at depth (Widiyantoro et al. 2018; Luehr et al. 2023, Chap. 5).

The activity of the Merapi dome was relatively calm and dominated by hydrothermal

activity in the period between 2015 and 2017. The UAS data added constraints to the study of the interaction between hydrothermal fluids and dome rocks that may strongly alter intact rocks, changing their porosity and permeability (Heap et al. 2019) by replacing the host rock minerals with secondary minerals and progressively reducing the strength of the dome rock (Pola et al. 2012; Wyering et al. 2014; Mayer et al. 2016). The location of hydrothermal activity was highly expressed at the structures of the Merapi dome, such as at the open NW–SE trending fissure and at the crescent-like structure described above. We hypothesised before that structural weakening at the crescent-like structure can trigger partial collapse at the southern dome sector without any significant seismic precursor in the future. Factor of safety analysis based on UAS data acquired at the southern dome sector suggests that intense rainfall at Merapi summit can further trigger this effect (Darmawan et al. 2018b). Indeed, this site was then also the location of collapses of the new dome that occurred in 2018–2019, as shown by 2019 UAS data (Fig. 15.5) and terrestrial photogrammetry datasets (Darmawan et al. 2020b, c).

The summary of the findings in this chapter are based entirely on drone-based photogrammetry, digital elevation modelling and analysis of the changes that occurred between UAS surveys. We note that, as UAS become more efficient, they may be able to carry instruments for measuring temperature (Zorn et al. 2020), gases become detectable and quantifiable (Liu et al. 2019), magnetic instruments may be deployed and picked up (Ohminato et al. 2011) and many further possibilities will arise (Jordan 2019; James et al. 2020). In addition, the use of more efficient image analysing methods such as classifiers, principal component analysis (Müller et al. 2021) and data science will further improve our ability to interpret data and understand volcanoes (Kereszturi et al. 2018).

In this regard, the use of UAS may allow much improved monitoring of hazards associated with dome building activity. Additionally, during periods of quiescence, the effects of hydrothermal

activity may be assessed using drone data. Hydrothermal activity and alteration will not only weaken the dome rock as the altered minerals accumulate and (Heap et al. 2019). This is potentially detectable in UAS imagery, as suggested by Kereszturi et al. (2018). The effects of hydrothermal alteration are important for hazard assessment, as they are associated with a possible reduction of rock strength, porosity and permeability, which can trigger superficial gas overpressure and may lead to a phreatic eruption (Stix and de Moor 2018). The full meaning of these alteration effects and possible interactions are still not fully understood at Merapi and elsewhere. However, we speculate that these may contribute to the explanation of the series of steam-driven explosions that suddenly occurred at Merapi between 11 May and 1 June 2018, possibly displaying a systematic change that occurs prior to renewed magmatic activity phases.

The UAS data presented have revealed details of a new dome growth episode, initiating at the open fissure in August 2018. The morphology of the new lava dome was first elongated, and strongly confined to and controlled by the open fissure. Of interest is that with continued extrusion of magma, this pre-defined direction waned. The dome grew endogenously in a relatively symmetric horizontal direction with an extrusion rate of 2200 m³/day and a low intensity of degassing as recorded by time lapse camera of the observatory (see published BPPTKG YouTube channel video; <https://www.youtube.com/c/BPPTKGCHANNEL>). The episode of dome growth reached its maximum volume of ~0.5 10⁶ m³ (BPPTKG 2019) and was in more depth investigated by Kelfoun et al. (2021), suggesting that total eruption volume may be much higher. The volume seen was affected by frequent gravitational collapses to the south, so that the erupted volume was estimated between 0.85 and 1.25 × 10⁶ m³, twice as large as the volume of the lava dome (Kelfoun et al. 2021). Exogenous extrusion may also occur during endogenous dome expansion, as indicated by our 2019 drone aerial images that recorded a blocky surface consisting of discrete lava lobes (Fig. 15.5b).

The endogenous-exogenous dome extrusion is quite common at dome-building volcanoes worldwide, such as Unzen volcano, Japan (Nakada et al. 1995; Kaneko et al. 2002), Soufrière Hills Volcano, Montserrat (Hale 2008), and the Santiaguito lava dome, Guatemala (Rhodes et al. 2018). We infer that endogenous—exogenous mechanisms were possible due to changes in magma rheology during dome growth. Exogenous domes will cool faster and become more viscous, whereas endogenous domes may stay insulated and retain a lower viscosity to outgas more efficiently and deflate (Kennedy et al. 2016).

As the dome continuously grows due to magma extrusion, it develops fractures, discrete dome lobes and oversteepening on its sides. Therefore, this mechanism of instability is characteristic for Merapi-type gravitational dome collapses (Voight et al. 2000), where the new UAS data suggest a strong control of pre-existing structures. In other words, by UAS surveys of the dome morphology and structural analysis, the processes and styles of later dome-building activity can be better understood.

15.5 Summary and Outlook

The morphology of the Merapi lava dome has significantly changed from 2012 to 2019. During this period, the dome underwent several profound morphological and structural changes, including (i) formation of a deep NW–SE trending fissure during the 2012–2014 steam-driven explosions, (ii) a period of hydrothermal activity and alteration, and (iii) renewed activity, initiated by explosions in 2018 followed by dome extrusion located inside the NW–SE trending fissure. Processes and hazards related to these morphological and structural changes and how they evolve can be well investigated by using UAS. The UAS data reveal that structures develop and evolve, possibly controlling later activity, sites of eruptions, flank instability and associated hazards. Moreover, with developing methods of the aircrafts, including the possibility to carry new sensors, and improved image

analysis and data science, it can be expected that the geomorphological and structural analysis of Merapi volcano and our understanding of associated hazards will significantly improve in the future.

Acknowledgements We appreciate support and suggestions by our colleagues in the office and in the field. We especially thank Professor Kirbani Sri Brotopuspito (†2019) for his vision and support of unconventional methods early during their development. We will miss him.

References

- Ashwell PA, Kennedy BM, Edwards M, Cole JW (2018) Characteristics and consequences of lava dome collapse at Ruawahia, Taupo Volcanic Zone, New Zealand. *Bull Volcanol* 80:43
- Beauducel F, Cornet FH, Suhanto E, Duquesnoy T, Kasser M (2000) Constraints on magma flux from displacements data at Merapi volcano, Java Indonesia. *J Geophys Res Solid Earth* 105(B4):8193–8203
- BPPTKG (2018) Diskusi Scientific forum: Kajian Erupsi Freatik G. Merapi 11 Mei 2018. In: BPPTKG website, Yogyakarta
- BPPTKG (2019) Laporan Aktivitas Gunung Merapi Tanggal 25–31 Januari 2019. In: BPPTKG website, Yogyakarta
- Bronto S, Rahardjo W, Asmoro P, Ratdomopurbo A, Adityarani M, Permatasari A (2023) The Godean debris avalanche deposit from a sector collapse of Merapi volcano. In: Gertisser R, Troll VR, Walter TR, Nandaka IGMA, Ratdomopurbo A (eds) *Merapi volcano—geology, eruptive activity, and monitoring of a high-risk volcano*. Springer, Berlin, Heidelberg, pp 195–231
- Calder ES, Lavallée Y, Kendrick JE, Bernstein M (2015) Lava dome eruptions. In: Sigurdsson H (ed) *The encyclopedia of volcanoes*, 2nd edn, chap 18. Academic Press, Amsterdam, p 343–362
- Darmawan H, Walter TR, Richter N, Nikkoo M (2017) High resolution digital elevation model of Merapi summit in 2015 generated by UAVs and TLS. V. 2015. GFZ Data Services. <https://doi.org/10.5880/GFZ.2.1.2017.003>
- Darmawan H, Walter TR, Brotopuspito KS, Subandriyo NIGMA (2018a) Morphological and structural changes at the Merapi lava dome monitored in 2012–2015 using unmanned aerial vehicles (UAVs). *J Volcanol Geotherm Res* 349:256–267
- Darmawan H, Walter TR, Troll VR, Budi-Santoso A (2018b) Structural weakening of the Merapi dome identified by drone photogrammetry after the 2010 eruption. *Nat Hazards Earth Syst Sci* 18:3267–3281
- Darmawan H, Mutaqin BM, Wahyudi HA, Wibowo HE, Haerani N, Suryayadi M, Syarifudin S,

- Asriningrum W (2020a) Topography and structural changes of Anak Krakatau due to the December 2018 catastrophic events. *Indones J Geogr* 52:402–410
- Darmawan H, Yuliantoro P, Suryanto W, Rakhman A, Budi Santoso A (2020b) Deformation and instability at Merapi dome identified by high resolution camera. *IOP Conf Ser Earth Environ Sci* 500:012008
- Darmawan H, Yuliantoro P, Rakhman A, Budi Santoso A, Humaida H, Suryanto W (2020c) Dynamic velocity and seismic characteristics of gravitational rockfalls at the Merapi lava dome. *J Volcanol Geotherm Res* 404:107010
- Darmawan H, Troll VR, Walter TR, Deegan FM, Geiger H, Heap MJ, Seraphine N, Harris C, Humaida H, Müller D (2022) Hidden mechanical weaknesses within lava domes provided by buried high-porosity hydrothermal alteration zones. *Sci Rep* 12(1):3202. <https://doi.org/10.1038/s41598-022-06765-9>
- Derrien A, Peltier A, Villeneuve N, Staudacher T (2020) The 2007 caldera collapse at Piton de la Fournaise: new insights from multi-temporal structure-from-motion. *Volcanica* 3:55–65
- Favalli M, Fornaciari A, Nannipieri L, Harris A, Calvari S, Lormand C (2018) UAV-based remote sensing surveys of lava flow fields: a case study from Etna's 1974 channel-fed lava flows. *Bull Volcanol* 80:29
- Gomez C, Kennedy B (2018) Capturing volcanic plumes in 3D with UAV-based photogrammetry at Yasur Volcano—Vanuatu. *J Volcanol Geotherm Res* 350:84–88
- Hale AJ (2008) Lava dome growth and evolution with an independently deformable talus. *Geophys J Int* 174:391–417
- Harijoko A, Marliyani GI, Wibowo HE, Freski YR, Handini E (2023) The geodynamic setting and geological context of Merapi volcano in Central Java, Indonesia. In: Gertisser R, Troll VR, Walter TR, Nandaka IGMA, Ratdomopurbo A (eds) *Merapi volcano—geology, eruptive activity, and monitoring of a high-risk volcano*. Springer, Berlin, Heidelberg, pp 89–109
- Heap MJ, Troll VR, Kushnir ARL, Gilg HA, Collinson ASD, Deegan FM, Darmawan H, Seraphine N, Neuberg J, Walter TR (2019) Hydrothermal alteration of andesitic lava domes can lead to explosive volcanic behaviour. *Nat Commun* 10:5063
- James M, Carr B, D'Arcy F, Diefenbach A, Dietterich H, Fornaciari A, Lev E, Liu E, Pieri D, Rodgers M, Smets B, Terada A, von Aulock F, Walter T, Wood K, Zorn E (2020) Volcanological applications of unoccupied aircraft systems (UAS): developments, strategies, and future challenges. *Volcanica* 3:67–114
- Jordan BR (2019) Collecting field data in volcanic landscapes using small UAS (sUAS)/drones. *J Volcanol Geotherm Res* 385:231–241
- Kaneko T, Wooster MJ, Nakada S (2002) Exogenous and endogenous growth of the Unzen lava dome examined by satellite infrared image analysis. *J Volcanol Geotherm Res* 116:151–160
- Kelfoun K, Budi-Santoso A, Latchimy T, Bontemps M, Nurdien I, Beauceul F, Fahmi A, Putra R, Dahamna N, Laurin A, Rizal MH, Sukmana JT, Gueugneau V (2021) Growth and collapse of the 2018–2019 lava dome of Merapi volcano. *Bull Volcanol* 83:8
- Kennedy BM, Wadsworth FB, Vasseur J, Ian Schipper C, Mark Jellinek A, von Aulock FW, Hess K-U, Kelly Russell J, Lavallée Y, Nichols ARL, Dingwell DB (2016) Surface tension driven processes densify and retain permeability in magma and lava. *Earth Planet Sci Lett* 433:116–124
- Kereszturi G, Schaefer LN, Schleiffarth WK, Procter J, Pullanagari RR, Mead S, Kennedy B (2018) Integrating airborne hyperspectral imagery and LiDAR for volcano mapping and monitoring through image classification. *Int J Appl Earth Obs Geoinf* 73:323–339
- Liu EJ, Wood K, Mason E, Edmonds M, Aiuppa A, Giudice G, Bitetto M, Francofonte V, Burrow S, Richardson T, Watson M, Pering TD, Wilkes TC, McGonigle AJS, Velasquez G, Melgarejo C, Bucarey C (2019) Dynamics of outgassing and plume transport revealed by proximal unmanned aerial system (UAS) measurements at Volcán Villarrica, Chile. *Geochem Geophys Geosyst* 20:730–750
- Luehr BG, Koulakov I, Suryanto W (2023) Crustal structure and ascent of fluids and melts beneath Merapi: insights from geophysical investigations. In: Gertisser R, Troll VR, Walter TR, Nandaka IGMA, Ratdomopurbo A (eds) *Merapi volcano—geology, eruptive activity, and monitoring of a high-risk volcano*. Springer, Berlin, Heidelberg, pp 111–135
- Malawani MN, Handayani T, Bariq JM, Lukafiardi R (2020) Morphological changes due to anthropogenic interferences in Gendol River Valley, Merapi Volcano. *Forum Geogr* 33:209–218
- Mayer K, Scheu B, Montanaro C, Yilmaz TI, Isaia R, Aßbichler D, Dingwell DB (2016) Hydrothermal alteration of surficial rocks at Solfatara (Campi Flegrei): petrophysical properties and implications for phreatic eruption processes. *J Volcanol Geotherm Res* 320:128–143
- McGonigle AJS, Aiuppa A, Giudice G, Tamburello G, Hodson AJ, Gurrieri S (2008) Unmanned aerial vehicle measurements of volcanic carbon dioxide fluxes. *Geophys Res Lett* 35:L06303
- Müller D, Walter TR, Schöpa A, Witt T, Steinke B, Gudmundsson MT, Dürig T (2017) High-resolution digital elevation modeling from TLS and UAV campaign reveals structural complexity at the 2014/2015 Holuhraun Eruption Site, Iceland. *Front Earth Sci* 5:59
- Müller D, Bredemeyer S, Zorn E, De Paolo E, Walter TR (2021) Surveying fumarole sites and hydrothermal alteration by unoccupied aircraft systems (UAS) at the La Fossa cone, Vulcano Island (Italy). *J Volcanol Geotherm Res* 413:107208
- Nakada S, Miyake Y, Sato H, Oshima O, Fujinawa A (1995) Endogenous growth of dacite dome at Unzen volcano (Japan), 1993–1994. *Geology* 23:157–160
- Nakano T, Kamiya I, Tobita M, Iwahashi J, Nakajima H (2014) Landform monitoring in active volcano by

- UAV and SFM-MVS technique. *Int Arch Photogramm Remote Sens* 40:71–75
- Ohminato T, Kaneko T, Koyama T, Watanabe A, Takeo M, Iguchi M (2011) Upward migration of the explosion sources at Sakurajima volcano, Japan, revealed by a seismic network in the close vicinity of the summit crater. AGU Fall Meeting 2011, Abstract ID V41H-07
- Pola A, Crosta G, Fusi N, Barberini V, Norini G (2012) Influence of alteration on physical properties of volcanic rocks. *Tectonophysics* 566–567:67–86
- Rhodes E, Kennedy BM, Lavallée Y, Hornby A, Edwards M, Chigna G (2018) Textural insights into the evolving lava dome cycles at Santiaguito lava dome Guatemala. *Front Earth Sci* 6:30
- Rokhmiana CA, Andaru R (2016) Utilizing UAV-based mapping in post disaster volcano eruption. 6th Insat Ann Eng Sem (InAES):202–205
- Stix J, de Moor JM (2018) Understanding and forecasting phreatic eruptions driven by magmatic degassing. *Earth Planets Space* 70:83
- Surono JP, Pallister J, Boichu M, Buongiorno MF, Budisantoso A, Costa F, Andreastuti S, Prata F, Schneider D, Clarisse L, Humaida H, Sumarti S, Bignami C, Griswold J, Carn S, Oppenheimer C, Lavigne F (2012) The 2010 explosive eruption of Java's Merapi volcano-A '100-year' event. *J Volcanol Geotherm Res* 241–242:121–135
- Syahbana DK, Kasbani K, Suantika G, Prambada O, Andreas AS, Saing UB, Kunrat SL, Andreastuti S, Martanto M, Kriswati E, Suparman Y, Humaida H, Ogburn S, Kelly PJ, Wellik J, Wright HMN, Pesicek JD, Wessels R, Kern C, Lisowski M, Diefenbach A, Poland M, Beauducel F, Pallister J, Vaughan RG, Lowenstern JB (2019) The 2017–19 activity at Mount Agung in Bali (Indonesia): intense unrest, monitoring, crisis response, evacuation, and eruption. *Sci Rep* 9:8848
- Szeliski R (2010) *Computer vision: algorithms and applications*, p 979
- Troll VR, Deegan FM (2023) The magma plumbing system of Merapi: the petrological perspective. In: Gertisser R, Troll VR, Walter TR, Nandaka IGMA, Ratdomopurbo A (eds) *Merapi volcano—geology, eruptive activity, and monitoring of a high-risk volcano*. Springer, Berlin, Heidelberg, pp 233–263
- Voight B, Constantine EK, Siswoidjoyo S, Torley R (2000) Historical eruptions of Merapi volcano, Central Java, Indonesia, 1768–1998. *J Volcanol Geotherm Res* 100:69–138
- Wahyudi SA, Putra H, Darmawan H, Suyanto I, Meilano I, Irzaman EM, Djamal M, Yasin M, Aminah NS, Perdinan AR, Srigutomo W, Suryanto W (2020) Topography changes and thermal distribution at the Kelud crater after the 2014 Plinian eruption. *Indones J Geogr* 52:411–417
- Walter TR (2023) Radar sensing of Merapi volcano. In: Gertisser R, Troll VR, Walter TR, Nandaka IGMA, Ratdomopurbo A (eds) *Merapi volcano—geology, eruptive activity, and monitoring of a high-risk volcano*. Springer, Berlin, Heidelberg, pp 437–455
- Walter TR, Salzer J, Varley N, Navarro C, Arámbula-Mendoza R, Vargas-Bracamontes D (2018) Localized and distributed erosion triggered by the 2015 Hurricane Patricia investigated by repeated drone surveys and time lapse cameras at Volcán de Colima, Mexico. *Geomorphology* 319:186–198
- Walter TR, Subandriyo J, Kirbani S, Bathke H, Suryanto W, Aisyah N, Darmawan H, Jousset P, Luehr BG, Dahm T (2015) Volcano-tectonic control of Merapi's lava dome splitting: the November 2013 fracture observed from high resolution TerraSAR-X data. *Tectonophysics* 639:23–33
- Watson M, Chigna G, Wood K, Richardson T, Liu E, Schellenberg B, Thomas H, Naismith A (2017) On the use of UAVs at active volcanoes: a case study from Volcan de Fuego, Guatemala. AGU Fall Meeting 2017, Abstract ID NH31C-03
- Watts RB, Herd RA, Sparks RSJ, Young SR (2002) Growth patterns and emplacement of the andesitic lava dome at Soufrière hills volcano, Montserrat. *Geol Soc Lond Mem* 21:115–152
- Widiyantoro S, Ramdhan M, Metaxian JP, Cummins PR, Martel C, Erdmann S, Nugraha AD, Budi-Santoso A, Laurin A, Fahmi AA (2018) Seismic imaging and petrology explain highly explosive eruptions of Merapi volcano Indonesia. *Sci Rep* 8:13656
- Wyering LD, Villeneuve MC, Wallis IC, Siratovich PA, Kennedy BM, Gravley DM, Cant JL (2014) Mechanical and physical properties of hydrothermally altered rocks, Taupo volcanic zone, New Zealand. *J Volcanol Geotherm Res* 288:76–93
- Zorn E, Walter T, Johnson BJ, Mania R (2020) UAS-based tracking of the Santiaguito lava dome Guatemala. *Sci Rep* 10:8644